Dalton Transactions

Accepted Manuscript

ROYAL SOCIETY OF CHEMISTRY

www.rsc.org/dalton

The novel two homologous phthalocyanine(Pc) series (azo- and oxo-bridged) substituted with 5-bromo-2-methoxyphenyl moiety were synthesized and characterized. The physical and chemical properties of the Pcs compared with each other for the first time. The ac response of the Pcs was also studied by impedance measurements over the temperature range of 300-500 K. Measurements showed that the dielectric permittivity of azo-bridged phthalocyanines is significantly higher than oxo-bridged homologs. This result can be attributed to the less electron delocalization ability of oxo-bridged homologs.

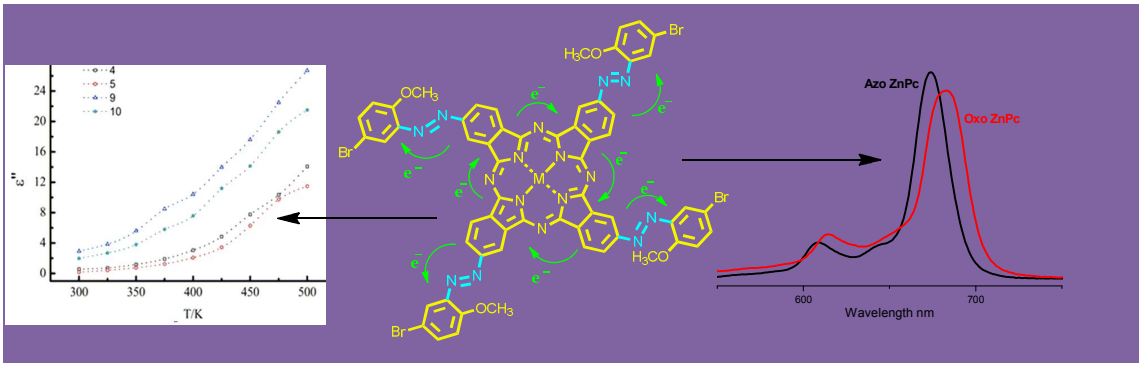

Cite this: DOI: 10.1039/c0xx00000x

www.rsc.org/xxxxxx

ARTICLE TYPE

Dielectric properties and electronic absorption: a comparison of novel azo- and oxo-bridged phthalocyanines

M. Merve Yüzüak,[a] Selçuk Altun,*[a] Ahmet Altındal[b] and Zafer Odabaş[a]

Received (in XXX, XXX) Xth XXXXXXXXX 20XX, Accepted Xth XXXXXXXXX 20XX
DOI: 10.1039/b000000x

The novel two homologous phthalocyanine (Pc) series (azo- and oxo-bridged) substituted with 5-bromo-2-methoxyphenyl moiety were synthesized and characterized. The physical and chemical properties of the Pcs compared with each other for the first time. The ac response of the Pcs was also studied by impedance measurements over the temperature range of 300-500 K. The real and imaginary parts of the impedance were found to be dependent on both frequency and temperature. Impedance spectra of the samples displayed semicircular arcs in the complex plane plot at all temperatures, with their centres lying below the real axis at a particular angle of depression indicating distribution of relaxation times. Measurements showed that the dielectric permittivity of azo-bridged phthalocyanines is significantly higher than oxo-bridged homologs. This result can be attributed to the less electron delocalization ability of oxo-bridged homologs.

1. Introduction

Phthalocyanines (Pcs) are a class of macrocyclic compound possessing a highly conjugated π-electron system, with intense absorption in the red/near-IR (Q band) region.[1] They display a number of unique properties, such as increased stability, architectural flexibility, diverse coordination properties, and improved spectroscopic characteristics,[2] which make them of great interest in various scientific and technological areas. It is well known that the properties of Pcs can be modified by changing the central metal ion and/or number, position, and character of substituents on the macrocycle.[3,4] Most of the applications of Pcs arise from their characteristic π-conjugation systems and their intense absorption in the red/IR region (Q-band).[5-7] Pcs are increasingly being employed in various devices, such as thin film flexible transistors, light emitting diodes, solar cells, rectifying devices and gas sensors.[8-13] The application of Pc compounds for the above devices is related to the electrical conductivity and dielectric relaxation process in the Pcs compounds and these are often the decisive factors about the suitability of the material for a particular device application. Therefore, the extraction of the true intrinsic nature of the electrical conduction and relaxation mechanism is essential for these materials. The basic electrical properties of many metal phthalocyanines (MPcs) have been studied in some details by various workers in the form of both single crystal and thin film.[14-16] Although a considerable body of data exists for dc and ac electrical characterization of Pcs, comparatively very little work has been carried out on the dielectric measurements for electrical transport phenomena of these materials.

In particular, while the oxo-bridged Pcs have been extensively investigated, little attention has been paid to their azo-bridged counterparts[17-20]. Indeed, except for Pcs, extended the conjugation length, neither electron-with drawing nor electron-donating substituent on conventional Pcs can show dramatic changes of electron density on Pc core due to limiting conjugation by oxo-bridge. Pcs, extended the conjugation length by conjugation across the bridges[21-23], can lead to superior performance in materials chemistry due to electron transfer from substituent to Pc core or vice versa. One of the principal strategies for changing of electron density on Pc core is simply to extend the conjugation length via azo bridged unit. Previos study has revealed that azo-bridged Pcs with electron donating group also exhibit more sensitive to toluene vapour according to oxo-bridged Pcs[24]. We wondered how to azo-bridged Pcs with electron withdrawing group (as bromine) affect the physical and electronic properties as compared with oxo-bridged Pcs. Hence, we have focused on the comparing of azo- and oxo-bridged Pcs' physical and electronic properties. Thus we can define and better understand the influence of "conjugated bridge" between Pcs core and the substitutients.

The present study contains two parts. In the first part, we synthesized (E)-4-((5-bromo-2-methoxyphenyl)diazenyl)phthalonitrile (**3**) and its azo-bridged Pc compounds (**4** and **5**) were also prepared. In the second part, 4-(5-bromo-2-methoxyphenoxy)-

phthalonitrile (**8**) and its oxo-bridged Pcs (**9** and **10**) were synthesized (Scheme 1). Finally, the physical and chemical properties of two homologous Pcs were compared with each other. Impedance spectroscopy technique was used to characterize the electrical properties of the films of **4**, **5**, **9**, and **10**. Temperature dependent measurements revealed that the operating temperature has a considerable effect on the impedance spectra of the films.

2. Experimental

2.1. Synthesis and characterization

The starting materials **3** and **8** were synthesized respectively according to the procedure described previously in the literature.[17,25] Compounds **1**, **2**, **6**, **7**, and $Zn(OAc)_2.2H_2O$ were purchased from Aldrich Chemical Co., and were used as received. All solvents were purified, dried and stored over molecular sieves. The Pc compounds were purified by washing in soxhlet system with an aqueous acetic acid (70%), water, and methanol, respectively. IR spectra were recorded on a Perkin Elmer Spectrum One FTIR (ATR sampling accessory) spectrophotometer. Electronic spectra were recorded on a Shimadzu UV-1601 spectrophotometer. Elemental analyses were performed by the Instrumental Analysis Laboratory of Tubitak–Ankara. ^{1}H-NMR spectra were recorded in deuterated dimethylsulfoxide (d-DMSO) using a Mercury-Vx 500 MHz instrument. Mass spectra were acquired on a Microflex III MALDI-TOF mass spectrometer (Bruker Daltonics, Germany) equipped with a nitrogen UV–Laser operating at 337 nm in reflectron mode with an average of 50 shots.

2.1.1. 4-((5-bromo-2-methoxyphenyl)diazenyl)phthalonitrile (3)

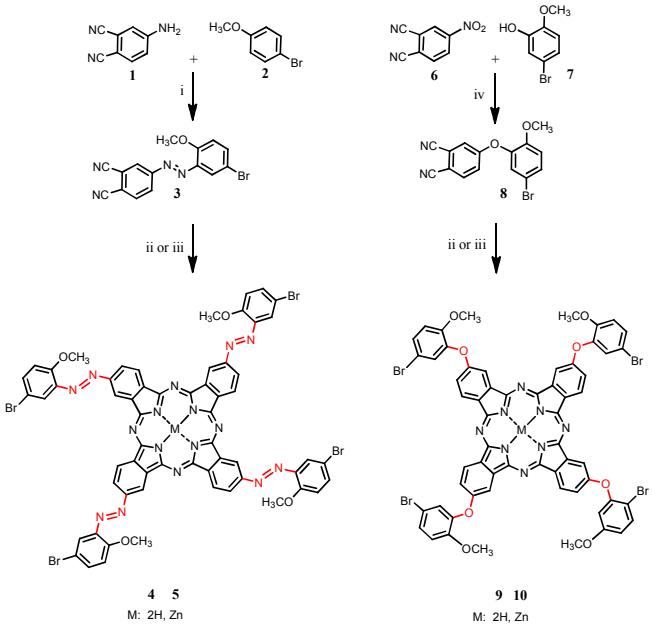

Scheme 1. Synthesis of compounds **3**, **4**, **5**, **8**, **9** and **10**. Reagents and conditions: (i) $NaNO_2$, HCl, 0-5°C, 24 hrs.; (ii) N_2, DMF, DBU, 350 °C, 15 min.; (iii) N_2, $Zn(CH_3COO)_2.2H_2O$, DMF, DBU, 350 °C, 15 min.; (iv) N_2, Na_2CO_3, DMSO, 50 °C, 48 hrs.

In a 50 mL Erlenmeyer flask, 10 mmol (1.4 g) 4-aminophthalonitrile (**1**) was dissolved in 6.5 mL concentrated HCl solution. The solution was cooled to 0-5° C in an ice bath and a solution of 11.6 mmol (0.8 g) $NaNO_2$ in 3.5 mL deionised water was slowly added. The mixture was stirred for 24 hours at 0 °C. A solution of 10 mmol (1.87 g) p-bromoanisole (**2**) in 4 mL glacial acetic acid was prepared and this solution was cooled in an ice bath then slowly added to the cold solution of the diazonium salt. The final reaction mixture was also stirred at 0 °C for 24 hours. The obtained red precipitate was filtered, washed with water, and dried. The crude product was purified by column chromatography with silica gel eluting with chloroform a gradient of chloroform- methanol from 0 to 5% methanol. Yield: 2.02 g (61%). This compound is soluble in tetrahydrofuran (THF), dimethylformamide (DMF), and DMSO. Mp: 135 °C. IR (KBr pellet) ν_{max}/cm^{-1}: 526, 771, 822, 847, 1020, 1140, 1171, 1207, 1241, 1267, 1326, 1385, 1460, 1483, 1497, 1574, 1591, 2233, 2843, 2943, 3044, 3081, 3108. Anal. Calc. for $C_{15}H_9BrN_4O$: C, 52.81; H, 2.66; N, 16.42. Found: C, 52.67; H, 2.85; N, 16.53%. ^{1}H-NMR (DMSO-d6) δ, ppm: 3.84 (s, 3H), 6.83 (d, J = 2.98 Hz, 1H), 6.89 (dd, J = 8.83 Hz, J = 3.00 Hz, 1H), 6.94 (d, J = 8.84 Hz, 1H), 7.41 (d, J = 2.46 Hz, 1H),7.53 (dd, J = 8.83 Hz, J = 2.48 Hz, 1H), 7.59 (d, J = 8.84 Hz, 1H).

2.1.2. 4-(5-bromo-2-methoxyphenoxy)phthalonitrile (8)

A mixture of 7.4 mmol (1.38 g) 4-nitrophthalonitrile (**6**) and 7.4 mmol (1.5 g) 5-bromo-2-methoxyphenol (**7**) was dissolved in 15 mL DMSO and 40 mmol (5.5 g) anhydrous K_2CO_3 was added into flask. The mixture was stirred at 40 °C under N_2 atmosphere for 2 days. At the end of this duration of time, reaction mixture was poured into 200 mL cold water. The white precipitate was filtered and washed with water, then dried. The crude product was purified by column chromatography with silica gel eluting with chloroform. Yield: 2.20 g (76%). This compound is soluble in THF, DMF, and DMSO. Mp: 138 °C. IR (KBr pellet) ν_{max}/cm^{-1}: 525, 624, 777, 802, 815, 844, 951, 1023, 1076, 1086, 1137, 1178, 1239, 1266, 1282, 1294, 1316, 1402, 1438, 1453, 1465, 1568, 1579, 1601, 2229, 2838, 2942, 3044, 3077, 3106. Anal. Calc. for $C_{15}H_9BrN_2O_2$: C, 54.74; H, 2.76; N, 8.51. Found: C, 54.63; H, 2.65; N, 8.69%. ^{1}H-NMR (chloroform-d) δ, ppm: 3.75 (s, 3H), 7.23 (d, J = 8.75 Hz, 1H), 7.30 (dd, J = 8.75 Hz, J = 2.45 Hz, 1H), 7.49 (d, J = 2.00 Hz, 1H), 7.50 (dd, J = 8.80 Hz, J = 2.15 Hz, 1H), 7.75 (d, J = 2.40 Hz, 1H), 8.05 (d, J = 8.80 Hz, 1H). ^{13}C-NMR ($CDCl_3$) (δ: ppm): 160.79, 150.59, 141.71, 136.08, 130.05, 125.21, 121.22, 120.56, 116.48, 115.86, 115.56, 115.34, 111.63, 107.94, 56.05.

2.1.3. General methods of syntheses of metal free-Pcs

A mixture of 0.14 g (0.4 mmol) compound **3** (or compound **8**) and 0.30 mL DMF and 0.05 mL 1,8-diazabicyclo[5.4.0] undec-7-ene (DBU) as catalyst were transferred in a reaction tube and then reaction mixture was heated for 10 minutes under dry N_2 atmosphere at 350 °C. After cooling the mixture to room temperature, 3 mL DMF was also added to solve the residue. The reaction mixture was precipitated by adding acetic acid. The precipitate was filtered and washed with an aqueous acetic acid solution (70%), water and methanol for 24 hours in a soxhlet apparatus, respectively. The crude product was purified by column chromatography with silica-gel eluted with a gradient of chloroform and THF.

2.1.3.1. (E)-2(3),9(10),16(17),23(24)-Tetra-((5-bromo-2-methoxyphenyl)diazenyl)phthalocyanine (4):

Yield: 0.065 g (47%). Solubility: THF, DMF and DMSO (weakly). Mp>350°C. IR (KBr pellet) ν_{max}/cm^{-1}: 524, 556,617, 718, 748, 832, 874, 1012, 1095, 1180, 1211, 1253, 1318, 1463, 1499, 1595, 1653, 2836, 2933, 3060, 3290. Anal. Calc. For $C_{60}H_{38}Br_4N_{16}O_4$: C, 52.73; H, 2.80; N, 16.40; Found: C, 52.64; H, 2.65; N, 16.59%.UV-*vis* (DMSO): λmax (nm) (log ε): 692 (5.017), 664 (5.013), 642 (4.854), 617 (4.772), 338 (5.036). ^{1}H-NMR (DMSO-d6): δ, ppm : 7.80–6.75 (m, 24H, aromatic), 3.81 (bs, 12H, $-OCH_3$), 1.52 (bs, 2H). m/z: 1255 $(M-OCH_3-Br)^+$, 1366 (M^+)

2.1.3.2. (3),9(10),16(17),23(24)-Tetra-(5-bromo-2-methoxy-phenoxy)phthalocyanine (9):

Yield: 0.089 g (67%). Solubility: THF, DMF and DMSO. Mp>350°C. IR (KBr pellet) ν_{max}/cm^{-1}: 741, 797, 930, 1009, 1091, 1130, 1177, 1212, 1262, 1295, 1321, 1396, 1473, 1579, 1614, 1666, 2835, 2939, 3066, 3288. Anal. Calc. For $C_{60}H_{38}Br_4N_8O_8$: C, 54.64; H, 2.90; N, 8.50. Found: C, 54.45; H, 2.75; N, 8.69%. UV-*vis* (DMSO): λmax (nm) (log ε): 700 (4.885), 672 (5.066), 636 (4.912), 612 (4.833), 341 (5.009). ^{1}H-NMR (DMSO-d6): δ, ppm : 8.10–7.10 (m, 24H, aromatic), 3.74 (bs, 12H, $-OCH_3$), 1.47 (bs, 2H). m/z: 1208 $(M-OCH_3-Br)^+$, 1319 $(M+H)^+$.

2.1.4. General methods of syntheses of ZnPcs

A mixture of 0.14 g (0.4 mmol) compound **3** (or compound **8**) and 0.13 g, (0.5 mmol) $Zn(CH_3COO)_2.2H_2O$ was transferred in a reaction tube. 0.30 mL DMF and 0.05 mL DBU as catalyst were added to the tube and then ZnPcs was synthesized according to above procedure.

2.1.4.1. 2(3),9(10),16(17),23(24)-Tetra-((5-bromo-2-methoxy-phenyl)diazenyl)phthalo-cyaninatozinc(II) (5):

Yield: 0.078 g (54%). Solubility: THF, DMF and DMSO. Mp>350°C. IR (KBr pellet) ν_{max}/cm^{-1}: 543, 626, 664, 723, 749, 800, 850, 880, 1050, 1092, 1126, 1185, 1293, 1307, 1336, 1380, 1422, 1442, 1498, 1600, 1650, 2893, 2926, 2973, 3064. Anal. Calc. for $C_{60}H_{36}Br_4N_{16}O_4Zn$: C, 50.39; H, 2.54; N, 15.67. Found: C, 50.48; H, 2.36; N, 15.57%. UV-*vis* (DMSO): λmax (nm) (log ε): 673 (5,180), 609 (4,431), 346 (4,662). ^{1}H-NMR (DMSO-d6): δ, ppm : 7.85–6.70 (m, 24H, aromatic), 3.82 (bs, 12H, $-OCH_3$). m/z: 1319 $(M-OCH_3-Br)^+$, 1430 (M^+), 1448 $(M+H_2O)^+$, 1466 $(M+2H_2O)^+$, 1484 $(M+3H_2O)^+$.

2.1.4.2. (3),9(10),16(17),23(24)-Tetra-(5-bromo-2-methoxy-phenoxy)phthalocyaninatozinc(II) (10):

Yield: 0.080 g (58%). Solubility: THF, DMF and DMSO. Mp>350°C. IR (KBr pellet) ν_{max}/cm^{-1}:743, 946, 1044, 1091, 1178, 1212, 1262, 1336, 1395, 1479, 1608, 1648, 2836, 2938, 3062. Anal. Calc. for $C_{60}H_{36}Br_4N_8O_8Zn$: C, 52.15; H, 2.63; N, 8.11. Found: C, 52.02; H, 2.75; N, 8.27%. UV-*vis* (DMSO): λ_{max} (nm) (log ε): 682 (5,155), 615 (4,578), 357 (4,901).). ^{1}H-NMR (DMSO-d6): δ, ppm : 8.08–7.14 (m, 24H, aromatic), 3.76 (bs, 12H, $-OCH_3$). m/z: 1272 $(M-OCH_3-Br)^+$, 1383 $(M+H)^+$.

2.2. Impedance measurements

The devices were fabricated on ordinary glass substrates. The glass substrates were cleaned by ultrasonic treatment in acetone, isopropyl alcohol, and deionized water before insertion into the deposition chamber. After surface cleaning, Au metal with high purity (99.99%) was thermally evaporated on the substrate at a pressure of $1x10^{-5}$ mbar in a thermal evaporation system (Edwards Auto 500). Pc thin films with a thickness of 400 nm were prepared by spin coating technique on Au coated glass substrates by a spin coating method at 1500 rpm using DMF as solvent. Au was selected as the electrode material, since it is well known that it forms an ohmic contact to the phthalocyanine. Spinning was continued for 120 s in order to allow the complete evaporation of the solvent, producing a uniform Pc film. Then the resulting films were heated at 95 °C for 1 h to ensure the removal of the residual solvent in the films. An elipsometric technique was used to measure the thickness of the Pc films. The error in the measurement of the thickness of the Pc films is estimated at about 1%. After the deposition of the Pc films, the substrate was immediately placed in a vacuum system for the top contact deposition processes. Circular dots of 1 mm in diameter and 1500 Å thickness Au contact were deposited on the top of the Pc layer through a metal shadow mask in a high vacuum system in a pressure of 1×10^{-5} mbar. Impedance measurements were carried out with an Agilent 4284A LCR meter in the frequency range of $100\text{-}2x10^6$ Hz and in the temperature range from 300 K to 500 K. The temperature of each sample was determined during the measurements using a pre-calibrated K-type thermocouple with an error of ± 0.1 K. All measurements were performed under vacuum ($\leq10^{-3}$ mbar) and in the dark. Impedance data were recorded on a PC using a GPIB data transfer card. The results were obtained under these conditions were reproducible with an uncertainty less than 2%.

3. Results and discussion

3.1. Synthesis and characterization

The starting compound **3** was synthesized in one step by azocoupling reaction of 4-aminophthalonitrile (**1**) with 4-bromoanisole (**2**) in nitrous acid solution generated in situ (in the same flask) from sodium nitrite and hydrochloric acid at 0-5 °C. The coupling reaction between **1** and **2** was regioselective resulting in the trans-form product. The regioselectivity arises from the fact that the resonance energy of the transform is approximately 3.5 kcal/mol lower than the cis-form.[26] The other starting compound **8** was synthesized by the nucleophilic aromatic substitution reaction of 4-nitrophthalonitrile (**6**) with 2-methoxy-5-bromophenol (**7**) (Scheme 1).

When a mixture of compound **3** (or **8**), $Zn(OAc)_2.2H_2O$ and DBU as a catalyst in absolute DMF was heated at approximately 350 °C for 15 min., compound **5** (or **10**) was isolated as a green precipitate. Pcs **4** and **9** were synthesized by using starting compound **3** and **8** respectively with the above procedure without metal salt. The spectroscopic data confirmed the proposed structures of the new compounds. The elemental analysis results for compounds **3**, **4**, **5**, **8**, **9**, and **10** were in good agreement with the calculated values.

The FT-IR absorption spectrum of **3** (and **8**) exhibited -C=C- double bond at 1591(1601) cm^{-1}, $-CH_3$ at 2845, 2942 (2838, 2942) cm^{-1} and stretching frequencies Ar-H at 3044, 3081 and 3108 (3044, 3077 and 3106) cm^{-1}. The appearance of a new absorption bands at 1483, 1497cm^{-1} -N=N- (1294 and 1316 cm-1 Ar-O-Ar) confirmed the formation of **3** (and **8**). The IR-spectra of the metal-free Pcs **4**, **9** and the zinc Pcs **5**, **10** were very similar, with the exception of metal-free Pcs **4** and **9** showing an extra N-H weak stretching band due to the inner core at 3290 and 3288

cm^{-1}, respectively and the sharp intense CN vibrational bands at 2233 and 2229 in the IR spectra of **3** and **8** also disappeared (Table 1).

The ^{1}H-NMR spectra of **3** (and **8**) exhibited characteristic signals for methoxy (-OCH_3) protons at 3.84 (3.75) ppm, as a singlet. The peaks at 6.83-6.94 (7.23-7.49) and 7.41-7.59 (7.50-8.05) ppm indicated the presence of the aromatic protons at the methoxybenzene and cyanobenzene rings, respectively.

The UV–*vis* spectra of metal-free (**4** and **9)**, and zinc Pcs (**5** and **10**) exhibited characteristic B and Q bands 337-355 nm and 656-700 nm, respectively (Table 2). The electron delocalization on the Pc molecules is affected strongly by the type of the bridge (oxo or azo) and the type of substituent which has the electron-withdrawing and electron-donating groups. In our previous study, the azo-bridged Pcs substituted with electron-donating group (dimethoxy group) showed a red shift of 3-5 nm according to oxo-bridged homologs.[24] In the present study, the UV–*vis* spectra of azo- (**4**, **5)** and oxo- (**9**, **10)** bridged Pcs were compared with each other, the spectra of azo-bridged Pcs showed a blue shift of 7-9 nm (Fig. 1 and 2). Thus, we observed that , the azo-bridged Pcs substituted with electron-donating group (dimethoxy group)[24] showed a shift of 10-14 nm according to the electron-withdrawing homolog. Similarly, Q band absorption of the azo-bridged Pcs substituted with electron-donating group (dihexylamino) showed at 736-746 nm in study of Y.-F. Li et al[18] and that of the azo-bridged Pcs substituted with electron-withdrawing group (carboxyl) and electron-donating group (carboxylate and dimethylamino) showed at 703-711 nm in study of Y. Liu et al[20]. In Liu's study, they discussed electron transfer from azobenzene π* orbital to phthalocyanine S_1 orbital for the first time by fluorescence spectroscopy and cyclic voltammetry.

Table 2 UV–*vis* spectral data for $1.0x10^{-5}$ mol dm^{-3} **4**, **5**, **9** and **10** in DMSO.

Pcs	Q-band λmax/nm (Log ε)	Vibration-band λmax/nm (Log ε)	B-band λmax/nm (Log ε)
Azo-2HPc (**4**)	692 (5.017) 664 (5.013)	642 (4.854) 617 (4.772)	338 (5.036)
Oxo-2HPc (**9**)	700 (4.885) 672 (5.066)	636 (4.912) 612 (4.833)	341 (5.009)
Azo-ZnPc (**5**)	673 (5.180)	609 (4.431)	346 (4.662)
Oxo-ZnPc (**10**)	682 (5.155)	615 (4.578)	357 (4.901)

The results suggest that π-π* transition energy from the highest occupied molecular orbital (HOMO) to the lowest unoccupied molecular orbital (LUMO) of the Pc ring increases due to the enhanced electron delocalization in the azo-bridged Pcs. The reason for the increase in the transition energy can be explained by electron withdrawing bromine group on the azo-bridged Pc rings (**4**, **5).** The effect of bromine group on oxo-bridged Pcs (**9**, **10)** was limited as the bridge breaks the electron delocalization. Aggregation behaviour of **4** and **9** was also examined by the spectra monitored at different concentrations within the range of $0.2x10^{-5}$ to $1.6x10^{-5}$ mol dm^{-3} in DMSO with the aim of providing additional support for the formation of their aggregated species in this solvent. The presence of aggregated species was confirmed by the deviation from Beer–Lambert law (inset in Fig. S5 and S6 respectively)[27].

MALDI-TOF samples were prepared by mixing the appropriate complex (2 mg/mL in THF) with the matrix, α-cyano-4-hydroxycinnamic acid (10 mg/mL in THF) solution (1:20 v/v) in a 0.5 mL Eppendorf micro-tube. Finally 1 mL of this mixture was deposited on the sample plate, dried at room temperature, and then analyzed. The molecular or protonated ion peaks of 4, 5, 9 and 10 were observed at 1366, 1430, 1319, and 1383 Da, respectively. Beside the molecular or protonated ion peaks, $(M–OCH_3–Br)^+$ fragment (all Pcs) and H_2O adducts (Pc **5**) peaks were observed.

Table 1 The specific IR bands of the compounds (**3**, **4**, **5**, **8**, **9** and **10**)

The compounds	N−H stretch.	=C−H stretch.	$>CH_2$ stretch.	C≡N stretch.	C=N stretch.	C=C stretch.	N=N bend.	C−H bend.	C−O stretch.	C−N stretch.	C−C stretch.
Azo-Ligand (**3**)	–	3108 3081 3044	2943 2843	2233	–	1591 1574	1497	1483 1460	1326 1267	–	1020
Oxo-Ligand (**8**)	–	3106 3077 3044	2942 2838	2229	–	1601 1579	–	1465 1453 1438	1316 1282 1266	–	1086 1076 1023
Azo-2HPc (**4**)	3290	3060	2933 2836	–	1653	1595	1499	1463	1318 1253	1180	1095 1012
Oxo-2HPc (**9**)	3288	3066	2939 2835	–	1666	1614 1579	–	1473	1321 1262	1177 1130	1091 1009
Azo-ZnPc (**5**)	–	3064 3000	2973 2926 2893	–	1650	1600	1498	1442 1422	1336 1293	1185 1126	1092 1050
Oxo-ZnPc (**10**)	–	3062	2938 2836	–	1648	1608	–	1479	1336 1262	1178	1091 1044

3.2. Impedance spectroscopy

The impedance spectra of the films were systematically measured in the frequency range of 100–$2x10^6$ Hz for all samples at different fixed temperatures. Fig. 3 shows the variation of real and imaginary parts of the measured impedance for **9** at room temperature. The complex impedance $Z^*(\omega)$, can be represented

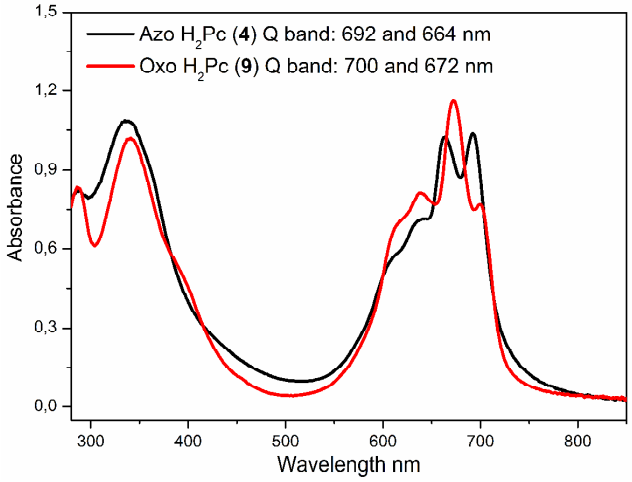

Fig. 1 UV–*vis* spectra of 1.0x10^{-5} mol.dm^{-3} the Pcs **4** and **9** in DMSO.

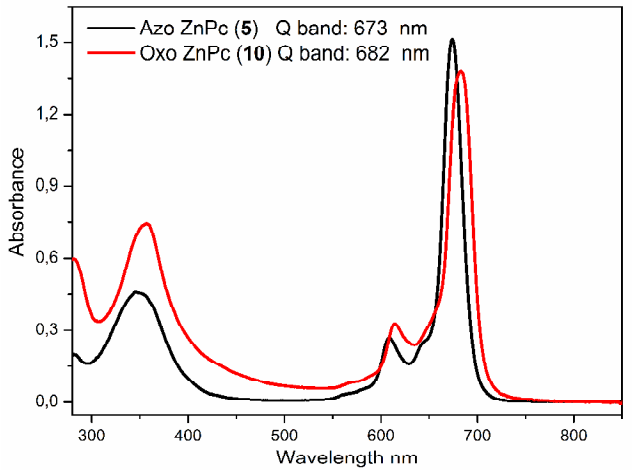

Fig. 2 UV–*vis* spectra of 1.0x10^{-5} mol.dm^{-3} the Pcs **5** and **10** in DMSO.

as a function of frequency as,

$$Z^*(\omega) = R + jX \quad (1)$$

where R and X are the real and imaginary parts of impedance. It can be seen from this figure that the magnitude of R decreases with the increase of frequency. The curves also display the single relaxation process and indicate an increase in ac conductivity with frequency.

The imaginary part of the complex impedance was found to increase with frequency for all samples at different frequencies, attaining a maximum value X_{max} and, thereafter, decreased. The X–log(f) curve also indicates the single relaxation process in the system. It was also observed that the frequency at which X_{max} occurred, called relaxation frequency, shifted to higher frequency regions as the temperature increased (Fig. 4). Similar temperature dependency of X was observed for other films (Fig. S1). The appearance and broadening of peaks at high temperatures suggest the presence of an electrical relaxation phenomenon in the materials. The relaxation process can be attributed to the

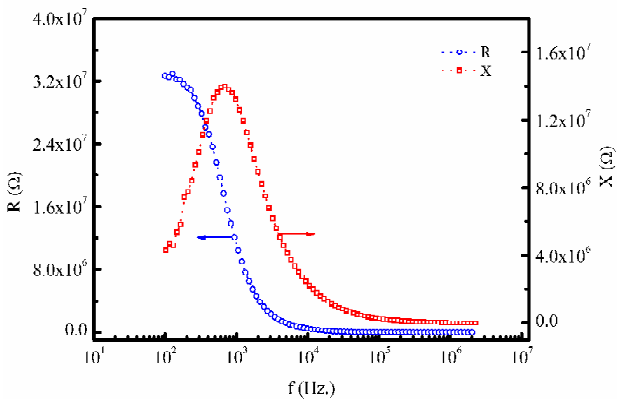

Fig. 3 Frequency dependence of the real and imaginary part of impedance at room temperature for **9**.

immobile species/electrons at low temperature and defects in the high temperature regions. According to Von Hipple,[28] the height of X peaks are proportional to bulk resistance (R_B) and can be expressed as,

$$X = R_B \frac{\omega\tau}{1+\omega^2\tau^2} \quad (2)$$

In this case, the relaxation is defined by the condition $\omega_{max}\tau_{max} = 1$ where τ_{max} is the relaxation time. It has been clearly observed that the relaxation frequency shifts to higher side with increasing temperature, resulting in lowering of relaxation time. In the case of where the mechanism responsible for conduction is hopping, the relaxation frequency is given by,[29]

$$\omega_{max} = \omega_0 \exp(-E_A / kT) \quad (3)$$

where ω_0 is the phonon frequency and E_A is the activation energy. The activation energy estimated for **4**, **5**, **9** and **10** are: 0.35, 0.38, 0.20 and 0.18 eV, respectively. Fig. 5 shows the measured complex impedance spectra (Cole–Cole plot) for the compound **9** recorded in the frequency range of 100–2x10^6 Hz at indicated temperatures. (For comparison, the room temperature impedance spectra for all Pcs is given in Fig.S2.) The impedance spectrum of 9 is characterised by the appearance of semicircle arcs whose pattern, contrary to its shape, changes when the temperature is

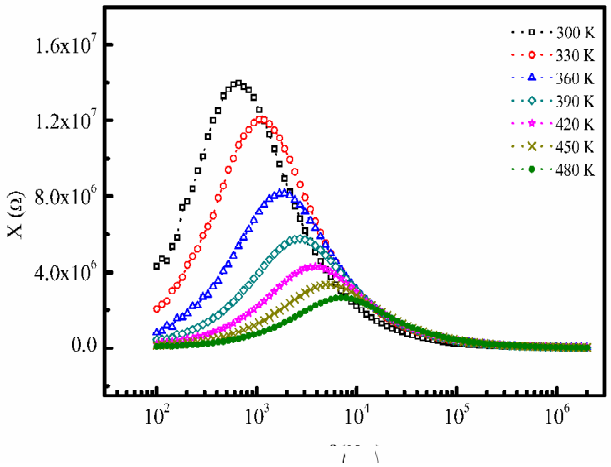

Fig. 4 The variation of imaginary part of impedance with temperature for **9**.

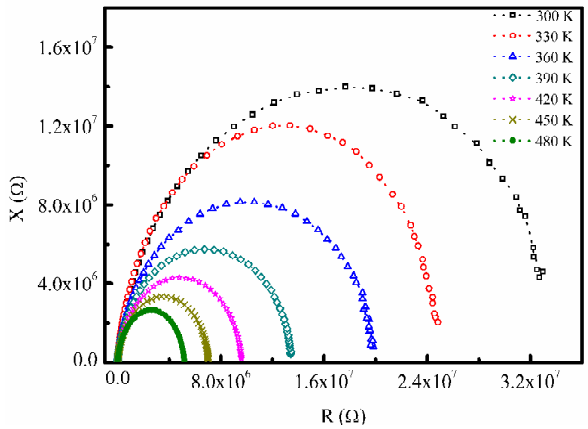

Fig. 5 Cole-Cole plot (X vs. R) of the sample of **9** at various temperatures.

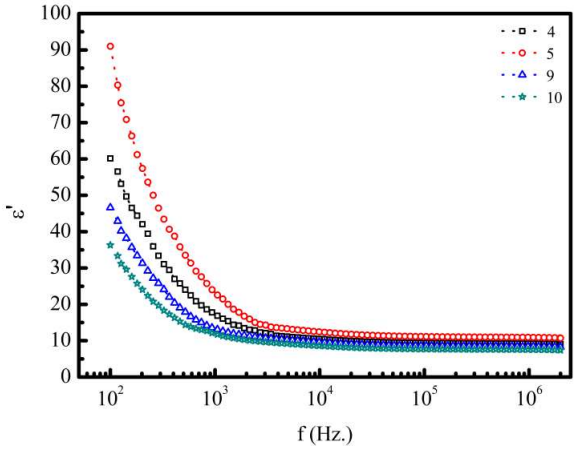

Fig. 6 Comparison of the dielectric constant of the compounds **4**, **5**, **9** and **10** at room temperature.

increased. Such a pattern tells us about the electrical processes occurring within the sample and their correlation with the sample microstructure when modelled in terms of an electrical equivalent circuit. An ideal semicircle in a complex plane plot appears only in Debye dispersion relation for a single relaxation time process. On the complex plane plot, only depressed semicircles with different radiuses were observed for all compounds, indicating deviation from the Debye dispersion relation. Depressed semicircles indicate that the maximum of the imaginary part of impedance is smaller than the half of the real part of impedance. The effect of temperature on the impedance spectra of the films becomes clearly visible with a rise in temperature. In the case of a depressed semicircle in the impedance spectra, the relaxation time is considered as a distribution of values, rather than a single relaxation time.

The impedance data are fitted well with a single depressed semicircle that gives a simple equivalent circuits of the device consisting of the parallel resistance (bulk resistance, R_B) and the constant phase element capacitance network in series with a series resistance (contact resistance).[30] The series resistance in the equivalent circuit represents the ohmic losses in the test fixture and electrode sheet resistance. The parallel resistance of the coating material is in parallel with that of the substrate. The presence of the constant phase element represents a slight distribution of relaxation times instead of a discrete relaxation time. This conclusion was supported by another type of Bode plot (log |Z| versus log |f|). The dependence of log |Z| versus log |f| shows slopes between -0.77 and -0.48 depending on temperature, which indicates the presence of a CPE. Similar results of the Bode plot were found for other compounds. The series resistance values extracted from the cole–cole plot is around 100 Ω for all the devices at room temperature.

Capacitance(C) and conductance (G) were systematically measured in the frequency range of 100–$2x10^6$ Hz for all samples at different fixed temperatures. The real, ε′(ω), and imaginary, ε"(ω), components of the complex dielectric function, ε*, were calculated from the relation,[30]

$$\varepsilon^* = \frac{1}{j\omega C_0 Z^*} = \varepsilon'(\omega) - j\varepsilon''(\omega) \quad (4)$$

where C and G are the measured capacitance and conductance of the sample, C_0 is the capacitance and of the empty measuring cell and ω is the angular frequency of the applied signal.

Fig.6 compares the variation of relative dielectric permittivity, ε′(ω), with frequency for the film of **4**, **5**, **9**, and **10** at room temperature. In all of the samples, a strong frequency dispersion of permittivity is observed in the low frequency region followed by a nearly frequency independent behavior. It was found that the general trend for the order of dielectric permittivity, observed in the whole temperature range for the investigated compounds is ε′ (**5**) > ε′ (**4**) > ε′ (**9**) > ε′ (**10**). The high values of ε′ for the **4** and **5** can be expected due to the long-range electron orbital delocalization in azo-bridged Pcs. When a field was applied, the probability of electron tunneling between molecules increases, resulting in a higher dielectric constant.[31] A similar variation of ε' with frequency is also observed at other temperatures.

For illustration, Fig. 7 (a) and (b) show the temperature and the frequency dependences of the real part of the complex dielectric function for the compound **9**. As shown in the figure, ε′ decreases monotonically with increasing frequency and attains a flat value at higher frequencies, and increases with the increasing temperature. It is also clear from Fig. 7 that the temperature dependence of ε′ is weak for higher frequencies. On the other hand, it exhibits relatively strong temperature dependence at the low frequency region. The other compounds have the same trend with the frequency and temperature. (Fig. S3 and Fig. S4) The increase in ε′ with temperature may be attributed to the electric field which is accompanied by applied frequencies. Such fields cause some ordering inside the samples as well as the formation of an electric moment in the entire volume of the dielectric and in each separate polarizing molecule. When the temperature rises, the dipoles orientation is facilitated, and this increases the dielectric constant. The temperature dependence of ε′ can be explained as follows: at relatively low temperatures, the dipoles on most cases cannot orient themselves with respect to the direction of the applied field, therefore, their contribution to the polarization and the dielectric constant are weak. As the temperature increases, the bound charge carriers get enough excitation thermal energy to be able to obey the change in the external field more easily. This in turn enhances their contribution to the polarization leading to an increase of the dielectric constant of the sample.[32]

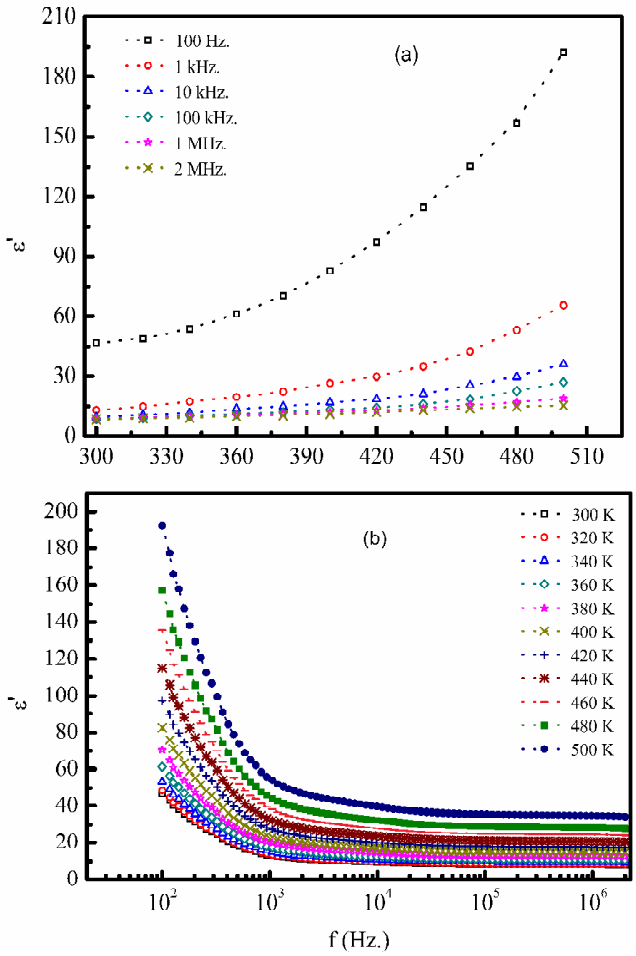

Fig. 7 The dependence of the dielectric constant, ε′, on (a) temperature (b) frequency for compound **9**.

A reasonable explanation for the observed frequency dependence of ε' can be given by following Koops's[33] theory, which is based on the Maxwell–Wagner model. In Koops's theory the solid is assumed to be composed of well conducting grains separated by highly resistive thin layers, grain boundaries. As a consequence of the applied signal to the sample, a space charge polarization is built up at the grain boundaries. The induced space charge polarization is controlled by the available free charges on the grain boundary and the conductivity of the sample. According to this model, the main contribution to the dielectric constant at low frequency comes from the grain boundaries, which have a high dielectric constant. On the other hand, at high frequency, the dielectric behavior of the sample is dominated by the grains which have a small dielectric constant. There is another additional aspect that should be recognized and accounted for the interpretation of the frequency dependence of ε′. At low frequency, the dipoles align themselves along the field direction and fully contribute to the total polarization. As the frequency is increased, the variation in the field becomes too rapid for the molecular dipoles to follow, so that their contribution to the polarization becomes less with a measurable lag because of internal frictional forces. The decrease of ε with the increase in frequency may be attributed to the electrical relaxation processes.

The imaginary components ε" of the dielectric function for all

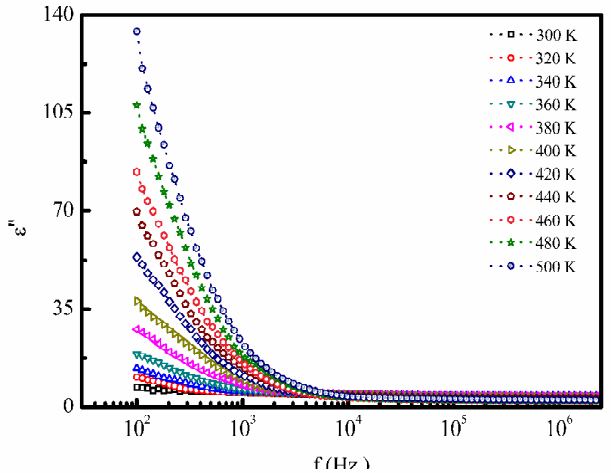

Fig.8 Frequency dependence of the dielectric loss ε"at various temperatures for **9**.

compounds in the same frequency and temperature ranges were also investigated. Fig. 8 shows the frequency dependence of ε" at different temperatures. As clearly seen from Fig. 8, no indication of a maximum peak is observed in ε" in the region of frequency dependence. Fig. 8 illustrates that ε" exhibits strong frequency dependence at higher temperatures and lower frequencies. At higher frequencies, the imaginary part of permittivity became less sensitive to both frequency and temperature. In the low frequency region, which corresponds to high resistivity due to the dominant effect of the grain boundaries at lower frequencies, more energy is required for hopping between the levels. Therefore the energy loss is high at lower frequencies. In the high frequency region, the required energy for electron transfer between the levels is small and hence the energy loss is small. The inverse frequency dependence of the imaginary dielectric constant at low frequencies was confirmation of the non-Debye type character of the overall relaxation. [34]

According to Stevels,[35] the origins of the dielectric loss are conduction losses, dipole losses, and vibrational losses. As the temperature increases, the electrical conduction losses increases which increases the dielectric loss ε".

4. Conclusions

In this study, the novel two homologous phthalocyanine series (azo- and oxo-bridged) were successfully synthesized and characterized. Their physical and chemical properties compared with each other for the first time. Impedance spectroscopy measurements were carried out on thin films of **4**, **5**, **9**, and **10** sandwiched between two evaporated Au electrodes. The measurements covered the temperature range of 300–500 K and a frequency range of 100 kHz to 2 MHz. The impedance spectra show strong temperature dependence in the investigated temperature and frequency ranges. The dielectric constant ε' and the dielectric loss ε" were found to decrease with increasing frequency and increase with increasing temperature. Such behaviour reveals that the tested compounds exist in the form of molecular dipoles. Our analysis based on the existing theories showed that the dielectric behaviour of the Pc compounds strongly depends on the kind of the bridging unit. The proposed study should include more refine investigation of the compounds including a wider temperature and frequency ranges.

Measurements showed that the dielectric permittivity of azo-bridged phthalocyanines is significantly higher compared to oxo-bridged homologs. This result can be explained as oxo-bridged homologs have less electron delocalization ability.

Acknowledgment

We are thankful to Marmara University, The Commission of Scientific Research Projects (BAPKO) (Project No: FEN-C-YLP-150513-0181 and FEN-A-130511-0159).

Notes and references

[a]*Department of Chemistry, Marmara University, 34722 Göztepe-Istanbul, Turkey. E-mail: merve.yuzuak@hotmail.com, selcukaltun@marmara.edu.tr, zodabas@marmara.edu.tr, Fax: +90 216 3478783; Tel: +90 216 3479641*

[b]*Department of Physics, Yildiz Technical University, Davutpasa Caddesi, 34220, Esenler, Istanbul, Turkey. E-mail: altindal@yildiz.edu.tr ; Fax: +90 212 383 42 34; Tel: +90 212 383 42 31*

1 P.Y. Reddy, L. Giribabu, C. Lyness, H.J. Snaith, C. Vijaykumar, M. Chandrasekharam, M. Gratzel, M.K. Nazeeruddin, *Angew. Chem. Int. Edit.,* 2007, **46**, 373.

2 K. Hanabusa, H. Shirai, *Phthalocyanines: Properties and applications* In: C. C. Leznoff, A.B.P. Lever (Eds.), VCH Publications, New York, 1993, vol. 2.

3 Y. Arslanoglu, E. Hayran, E. Hamuryudan, *Dyes Pigm.*, 2013, **97**, 340.

4 Z. Odabaş, E.B. Orman, M. Durmuş, F. Dumludağ, A.R. Özkaya, M. Bulut, *Dyes Pigm.,* 2012, **95**, 540.

5 C.G. Claessens, U. Hahn, T. Torres, *Chem. Rec.,* 2008, **8**, 75.

6 N.B. McKeown, I. Chambrier, M.J Cook, *Chem. Soc., Perkin Trans.*, 1990, **1**, 1169.

7 M.J. Cook, *Chem. Rec.,* 2002, **2**, 225.

8 Z. Bao, A.J. Lovinger, A. Dodabalapur, *Appl. Phys. Lett.*, 1996, **69**, 3066.

9 S.C. Kim, G.B. Lee, M.W. Choi, Y. Roh, C.N. Whang, K. Jeong, J.G. Lee, and S. Kim, *Appl. Phys. Lett.,* 2001, **78**, 1445.

10 S. Schumann, R.A. Hatton, and T.S. Jones, *J. Phys. Chem. C*, 2011, **115**, 4916.

11 Ü. Salan, A. Altındal, A.R. Özkaya, B. Salih and Ö. Bekaroğlu, *Dalton Trans.,* 2012, **41**, 5177.

12 A. Yazıcı, C. Özkan, M.B. Gezer, A. Altındal, B. Salih, Ö. Bekaroğlu, *Inorg. Chim. Acta,* 2013, **404**, 40.

13 Z. Odabaş, A. Altındal, A.R. Özkaya, B. Salih, Ö. Bekaroğlu, *Sens. Actuators B*, 2010, **145**, 355.

14 A. Altındal, Ş. Abdurrahmanoğlu, M. Bulut, Ö. Bekaroğlu, *Synth. Met.,* 2005, **150**, 181.

15 R.D. Gould, T.S. Shafai, *Thin Solid Films,* 2000, **373**, 89.

16 Y. Aoyagi, K. Masuda and S. Namba, *J. Phys. Soc. Jpn.,* 1971, **371**, 164.

17 Y.F. Li, S.L. Li, K.J. Jiang, L.M. Yang, *Chem. Lett.,* 2004**, 33,** 1450.

18 Y.-F. Li, T.-F. Jiao, *J. Dispersion Sci. Technol.*, 2007, **28**, 603.

19 X.A. Mico, S.I. Vagin, L.R. Subramanian,T. Ziegler, M. Hanack, *Eur. J. Org. Chem.,* 2005, 4328.

20 Y. Liu, H. Lin, X. Li, J. Li, H. Nan, *Inorg. Chem. Commun.,* 2010, **13**,187.

21 E.M. Maya, P. Vazquez, T. Torres, *Chem. Eur. J.* 1999, **5**, 2004.

22 L. Rintoul, S.R. Harper, D.P. Arnold, *Phys.Chem. Chem. Phys.,* 2013, **15**, 18951.

23 T.E.O. Screen, L.M. Blake, L.H. Rees, W. Clegg, S.J. Borwick, H.L. Andersona*, J. Chem. Soc., Perkin Trans. 1*, 2002, 320.

24 S, Şahin, S, Altun, A, Altındal, Z.Odabaş, *Sens. Actuators B*, 2015, **206**, 601.

25 Z. Odabaş, A. Altındal, B. Salih, M. Bulut, Ö. Bekaroğlu, *Polyhedron*, 2007, **26**, 695.

26 C. Krieger, A. Koçak, Ö. Bekaroğlu, *Helv. Chim. Acta,* 1985, **68**, 581.

27 I. Acar, Z. Bıyıklıoğlu, M. Durmuş, H. Kantekin, *J. Organomet. Chem.,* 2012, **65**, 708.

28 R. Von Hipple, *Dielectrics and waves*, John Wiley and Sons, New York, 1954.

29 M. Pollak, G.E. Pike, *Phys. Rev. Lett.,* 1972, **28**, 1444.

30 J.R. Macdonald, *Impedance spectroscopy, theory, experiment, and applications,* John Wiley & Sons, 2005.

31 H. Xu, Y. Bai, V. Bharti, Z.Y. Cheng, *J. Appl. Polym. Sci.,* 2001, **82**, 70.

32 M.R. Anantharaman, S. Sindhu, S. Jagatheesan, K.A. Molini, P. Kurian, *J. Phys. D: Appl. Phys.*, 1999, **32**, 1801.

33 C. Koops, *Phys. Rev.,* 1951, **83**, 121.

34 A.Yazıcı, N. Ünüş, A. Altındal, B. Salih, Ö. Bekaroğlu, *Dalton Trans.,* 2012, **41**, 3773.

35 J.M. Stevels, *Handbuch der physik,* in: S. Flugge (Ed.), Springer, Berlin, 1957, pp. 350.